Catalysis Science & Technology

Accepted Manuscript

ROYAL SOCIETY OF CHEMISTRY

www.rsc.org/catalysis

Journal Name

ARTICLE

A high-efficiency $CeWO_x$ catalyst for the selective catalytic reduction of NO_x with NH_3

Wenpo Shan,[a]* Yang Geng,[a] Xiaoling Chen,[a] Nan Huang,[a] Fudong Liu [b] and Shijian Yang [a]

Received 00th January 20xx,
Accepted 00th January 20xx

DOI: 10.1039/x0xx00000x

www.rsc.org/

In this study, two methods were used to prepare Ce-W oxide catalysts. A $CeWO_x$ catalyst prepared by homogeneous precipitation method showed excellent NH_3-SCR performance, with over 80% NO_x conversion obtained from 225 to 450 °C under a high GHSV of 300,000 h^{-1}. Characterizations revealed that the homogeneous precipitation method can achieve highly dispersed active species and intense interaction between Ce and W species on $CeWO_x$ catalyst, and thus results in enhanced charge imbalance, superior redox functions, and outstanding adsorption and activation properties for reactants, which is the main reason for the high efficient NO_x abatement of $CeWO_x$ catalyst.

1. Introduction

NO_x (NO and NO_2) are major air pollutants inducing acid rain, photochemical smog and haze and causing direct damages to the respiratory systems of human bodies. NO_x are mainly produced during the combustion of fossil fuels from stationary sources such as coal-fired power plants and mobile sources such as motor vehicles. In recent years, great efforts have been applied to the development and application of available technologies for the control of NO_x emissions.[1,2] Among these technologies, selective catalytic reduction of NO_x with NH_3 (NH_3-SCR: $4\ NO + 4\ NH_3 + O_2 \rightarrow 4\ N_2 + 6\ H_2O$), using vanadium-based catalysts, has been widely applied for the removal of NO_x generated from stationary sources since 1970s.[3] Three-way catalysts have already been successfully adopted for the simultaneous abatement of NO_x, CO, and unburned hydrocarbons from gasoline powered vehicles.[4] However, the emission of NO_x remains a major problem for diesel powered vehicles.[5]

In addition to stationary sources, NH_3-SCR has also been introduced into the market for diesel vehicles and is thought to be one of the best technologies for meeting the ever tightened emission standards.[6,7] Together with NH_3-SCR, vanadium-based catalysts, especially V_2O_5-WO_3/TiO_2, were also employed as the first generation of NH_3-SCR catalysts on diesel engines.[2,4,8] However, the toxicity of active vanadium species together with the narrow operation temperature window restrained the further applications of the V-based catalysts for diesel vehicles. Fe (or Cu)-exchanged zeolites, with superior NH_3-SCR performance under high space velocity conditions, have received increasing attention for the purpose of mobile application.[9] Starting from 1990s, great efforts have been made to ZSM-5 catalysts.[10,11] However, the insufficient low-temperature activity of Fe-ZSM-5 and the poor hydrothermal stability of Cu-ZSM-5 are still problems for their applications on diesel vehicles. Recently, Cu containing small pore zeolites, such as Cu-SSZ-13 [12,13] and Cu-SAPO-34 [14,15] with CHA structure and Cu-SSZ-39 [16] and Cu-SAPO-18 [17] with AEI structure, were shown to have very high activity and excellent hydrothermal stability and thus received much attention for the applications on diesel vehicles.[18-20]

Various transition metal (such as Fe [21], Cu [22], Mn [23,24] and Ce [25,26])-based vanadium-free oxide catalysts were also reported as potential substitutions of V-based catalyst. There are limitations to the catalyst volume that can be placed on board, which requires that the SCR catalyst should work efficiently under high space velocity conditions.[4] Nevertheless, the developed oxide catalysts were usually tested under relatively low space velocity conditions. In our previous study, we have successfully developed a series of Ce-based oxide catalysts for NH_3-SCR.[26-29] Among them, a Ce-W oxide catalyst showed very high efficiency for the reduction of NO_x emission from diesel exhaust.[30] In this study, we furtherly prepared the catalyst with different methods, characterized the catalyst using various techniques, and investigated the reason for the excellent NH_3-SCR performance of the catalyst.

2. Experimental

2.1 Catalyst synthesis and activity test

The Ce-W oxide catalyst was prepared by homogeneous precipitation method using cerium nitrate and ammonium tungstate as precursors. $(NH_4)_{10}W_{12}O_{41}$ and $Ce(NO_3)_3{\cdot}6H_2O$, with a Ce/W molar ratio of 1:1, were dissolved in oxalic acid solution, and then excessive urea was added into the solution.

---

[a] *School of Environmental and Biological Engineering, Nanjing University of Science and Technology, Nanjing 210094, PR China. E-mail: wenposhan@hotmail.com; Fax: +86 25 84315173; Tel: +86 18012920637.*

[b] *Materials Sciences Division, Lawrence Berkeley National Laboratory, Berkeley 94720, California, United States. Address here.*

Electronic Supplementary Information (ESI) available: Catalyst preparation by citric acid method, activity comparisons, effects of H_2O, N_2O formation analysis, and some characterizations. See DOI: 10.1039/x0xx00000x.

The mixed solution was heated to 90 °C and held there for 12 h under vigorous stir. After filtration and washing with deionized water, the resulting precipitant was dried at 100 °C overnight and subsequently calcined at 500 °C for 5 h in air condition. The obtained catalyst by this method was denoted as $CeWO_x$. Pristine CeO_2 and WO_3 were also prepared using the same method as reference samples.

Another Ce-W oxide catalyst was prepared by solution evaporating method using the same Ce and W precursors. $(NH_4)_{10}W_{12}O_{41}$ and $Ce(NO_3)_3·6H_2O$, with a Ce/W molar ratio of 1:1, were dissolved in oxalic acid solution, and then the water in the mixed solution was evaporated at 100 °C for 36 h. After that, the collected solid was calcined at 500 °C for 5 h in air condition. The obtained catalyst by this method was denoted as CeO_2-WO_3.

Before NH_3-SCR activity test, the powder catalysts were pressed, crushed and sieved to 40-60 mesh. The SCR activity tests of the sieved powder catalysts (0.08 mL) were carried out in a fixed-bed quartz flow reactor at atmospheric pressure. The reaction conditions were controlled as follows: 500 ppm NO, 500 ppm NH_3, 5 vol.% O_2, N_2 balance, and 400 mL/min total flow rate. The effluent gas, including NO, NH_3, NO_2 and N_2O was continuously analyzed by an online FTIR gas analyzer (Nicolet Antaris IGS analyzer). The concentration data were collected after 0.5 h when the SCR reaction reached a steady state.

2.2 Characterizations

The surface areas of the catalysts were obtained from N_2 adsorption/desorption analysis at -196 °C using a Micromeritics ASAP 2020. Prior to N_2 physisorption, the catalysts were degassed at 300 °C for 4 h. Surface areas were determined by BET equation in 0.05-0.35 partial pressure range.

Powder X-ray diffraction (XRD) measurements of the catalysts were carried out on a computerized PANalytical X'Pert Pro diffractometer with Cu Kα (λ = 0.15406 nm) radiation. The data of 2θ from 20 to 80 ° were collected at 8 °/min with the step size of 0.07 °.

The XPS of the catalysts were recorded on a Scanning X-ray Microprobe (Axis Ultra, Kratos Analytical Ltd.) using Al Ka radiation (1486.7 eV). The binding energies of Ce 3d, W 4f and O 1s were calibrated using C 1s peak (BE = 284.8 eV) as standard.

The H_2-TPR tests were carried out on a Micromeritics AutoChem_II_2920 chemisorption analyzer. The samples (100 mg) in a quartz reactor were pretreated at 400 °C in a flow of air (50 mL/min) for 1 h and cooled down to room temperature. Then H_2-TPR was performed in 10 vol % H_2/Ar gas flow of 50 mL/min at a heating rate of 10 °C/min.

The NO_x-TPD and NH_3-TPD were performed using the same reactor as activity tests. A typical experiment of NO_x-TPD used 600 mg sample and a gas flow rate of 200 mL/min. The experiment consisted of four stages: (1) degasification of the catalyst under N_2 at 350 °C for 1 h, (2) adsorption of 500 ppm NO and 5 vol.% O_2 at 50 °C for 1 h, (3) isothermal desorption under N_2 at 50 °C, and (4) temperature-programmed desorption under N_2 at 10 °C/min up to 500 °C. A typical experiment of NH_3-TPD used 100 mg sample and a gas flow rate of 200 mL/min. The experiment procedure of NH_3-TPD was similar with that of NO_x-TPD, but in stage (2) the adsorption was carried out under 500 ppm NH_3 condition.

3. Results and discussion

3.1 NH_3-SCR activity

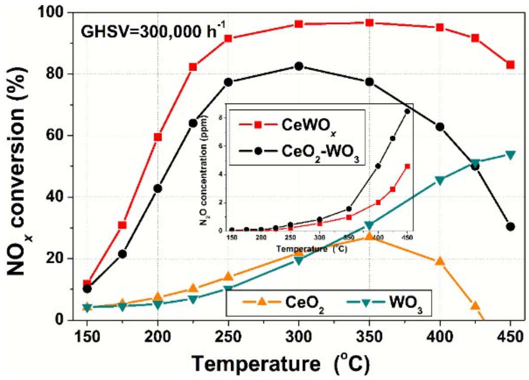

Fig. 1 NO_x conversions and N_2O productions (inserted) over the catalysts. Reaction conditions: [NO] = [NH_3] = 500 ppm, [O_2] = 5 vol.%, N_2 balance and GHSV = 300,000 h^{-1}.

Fig. 1 shows the NO_x conversion over the catalysts with different preparation methods under a high GHSV of 300,000 h^{-1}. Both pristine CeO_2 and WO_3 showed rather poor SCR activity in the whole temperature range. However, both the $CeWO_x$ catalyst (prepared by homogeneous precipitation method) and the CeO_2-WO_3 catalyst (prepared by solution evaporating method) exhibited much higher NH_3-SCR activity in a broad temperature range. This result indicates that a synergistic effect might exist between Ce species and W species for the NH_3-SCR reaction over $CeWO_x$ and CeO_2-WO_3 catalysts.

The CeO_2-WO_3 catalyst just presented good activity in the medium temperature range from 250 to 350 °C. Under the same space velocity condition, the $CeWO_x$ catalyst prepared by homogeneous precipitation method showed excellent activity in a broad temperature range, with over 80% NO_x conversion from 225 to 450 °C. Furthermore, the N_2O production during NH_3-SCR over $CeWO_x$ was lower than that over CeO_2-WO_3 (see the ESI† for details of the N_2O formation analysis). Compared with CeO_2-WO_3, the $CeWO_x$ catalyst was clearly more efficient for NO_x abatement, with higher NO_x conversion and lower N_2O production in the whole temperature range. In addition, a Ce-W oxide catalyst was also prepared by citric acid method.[31-33] However, this catalyst just showed rather low NO_x conversion in the whole temperature range (see the ESI† for details of this catalyst).

H_2O can significantly influence the catalytic performance of the NH_3-SCR catalysts.[34-36] Therefore, the effects of H_2O on the NO_x conversion over the $CeWO_x$ and CeO_2-WO_3 catalysts were further tested. The results indicated that the existence of 5% H_2O in the feed gas could induce a decrease of low temperature activity while an enhancement of high temperature activity. Over 80% NO_x conversion could still be obtained from 250 to 450 °C over the $CeWO_x$ catalyst (see the ESI† for details of the effects of H_2O).

3.2 Separated NO/NH_3 oxidation

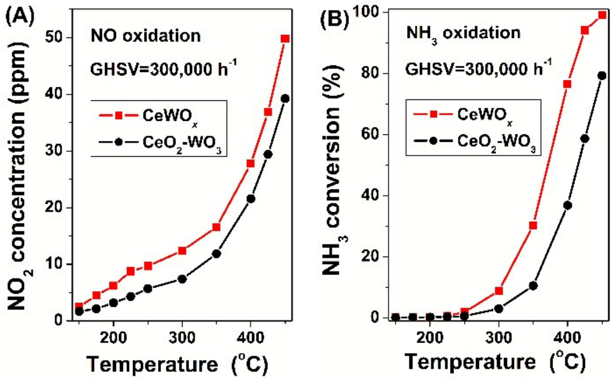

Fig. 2 (A) NO_2 productions during separate NO oxidation reaction and (B) NH_3 conversions during separate NH_3 oxidation reaction over $CeWO_x$ and CeO_2-WO_3 catalysts. Reaction conditions: (A) [NO] = 500 ppm, (B) [NH_3] = 500 ppm, [O_2] = 5 vol.%, N_2 balance and GHSV = 300,000 h^{-1}.

For low temperature NH_3-SCR, NO oxidation to NO_2 is very important to promote deNO_x efficiency by accelerating the ‘‘fast SCR’’ process ($2\ NH_3 + NO + NO_2 \rightarrow 2N_2 + 3H_2O$). If a catalyst can effectively oxidize NO to NO_2 *in situ* under NH_3-SCR conditions, the NO_x can be efficiently removed at low temperature.[36-38] In this study, separated NO oxidation tests were carried out over $CeWO_x$ and CeO_2-WO_3, and the NO_2 production during the tests were shown in Fig. 2(A). The low-temperature NO_2 production over $CeWO_x$ was clearly higher than that over CeO_2-WO_3, implying that $CeWO_x$ was more efficient for the oxidation of NO during NH_3-SCR reaction and thereby showed higher low-temperature SCR activity. In addition, as shown in Fig. 2(B) the NH_3 oxidation ability of $CeWO_x$ was also obviously higher than that of CeO_2-WO_3, while the formed N_2O over $CeWO_x$ was lower than that over CeO_2-WO_3 (see the ESI† for details of the N_2O formation).

3.3 BET surface area and XRD

Table 1 BET surface area, crystallite size and surface Ce/W atomic ratio of the catalysts

Sample	BET surface area (m^2/g)	Crystallite size (nm)		Surface Ce/W atomic ratio [a]
		CeO_2	WO_3	
$CeWO_x$	69.9	9.5	/	1.27
CeO_2-WO_3	39.8	9.9	18.8	1.03

[a] According to XPS analysis

As shown in Table 1, the BET surface area of $CeWO_x$ (69.9 m^2/g) was higher than that of CeO_2-WO_3 (39.8 m^2/g), which might be a reason for the higher NH_3-SCR activity of $CeWO_x$.

From the XRD results in Fig. 3, we can see that the coexistence of Ce and W species could inhibit the crystallization of CeO_2 and WO_3, which probably lead to much higher dispersion of active species. Both CeO_2 and WO_3 crystallites were detected in CeO_2-WO_3, while only CeO_2 crystallite was observed in $CeWO_x$. Compared with the diffraction pattern of pristine CeO_2, the intensities of CeO_2 crystallite for $CeWO_x$ and CeO_2-WO_3 both weakened. According to the calculations by Scherrer equation, the average crystallite size of cerianite CeO_2 in $CeWO_x$ is smaller than that in CeO_2-WO_3 (Table 1). Due to the significant difference between the ionic radii of Ce^{4+} (0.097 nm) and W^{6+} (0.062 nm), it is less likely to form a solid solution by incorporation of W^{6+} into the lattice of CeO_2. Considering the previously proposed structure of Ce-W oxides, such as that proposed by Peng et al., the W species in $CeWO_x$ probably existed as amorphous phase, or crystallite phase with very small particle size.[39] In such case, it is reasonable to see no clear diffraction peak of W species.

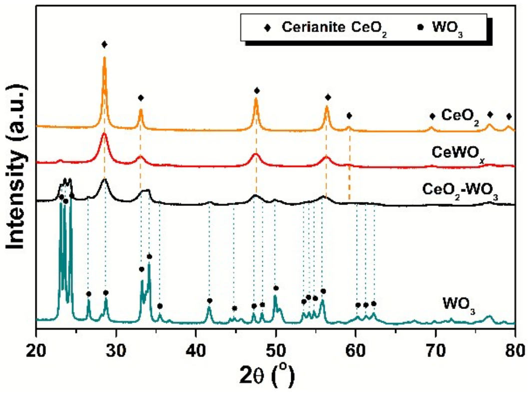

Fig. 3 XRD patterns of the catalysts.

3.4 XPS results of Ce 3d

The highly dispersed small CeO_2 crystallites has been identified as the main active sites for Ce-based catalysts. According to the XPS results, the surface Ce/W atomic ratio of $CeWO_x$ was clearly higher than that of CeO_2-WO_3 (Table 1), which indicates that the homogenous precipitation method could induce more abundant CeO_2 crystallite and thus increase the amount of active sites on the catalyst surface.

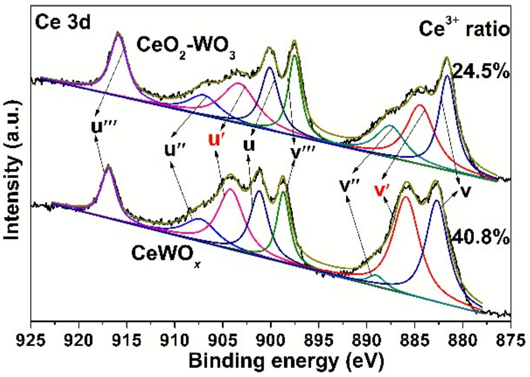

Fig. 4 XPS results of Ce 3d of $CeWO_x$ and CeO_2-WO_3 catalysts.

The Ce 3d peaks were fitted by searching for the optimum combination of Gaussian bands with the correlation coefficients (r^2) above 0.99 (Fig. 4). The sub-bands labelled u' and v' represent the $3d^{10}4f^1$ initial electronic state corresponding to Ce^{3+}, and the sub-bands labelled u, u'', u''', v, v'', and v''' represent the $3d^{10}4f^0$ state of Ce^{4+}. The Ce^{3+} ratio, calculated by $Ce^{3+}/(Ce^{3+} + Ce^{4+})$, of $CeWO_x$ (40.8%) was significantly higher than that of CeO_2-WO_3 (24.5%). The presence of Ce^{3+} could result in a charge imbalance, which would lead to oxygen vacancies and unsaturated chemical bonds and generate additional chemisorbed oxygen or weakly adsorbed oxygen species on the surface of catalyst.[40-42] The XPS results of O 1s of the $CeWO_x$ and CeO_2-WO_3 catalysts confirmed that the ratio of surface adsorbed oxygen (such as the O_2^{2-} and O^- belonging to defect-oxide or hydroxyl-like group) on $CeWO_x$ was higher than that on CeO_2-WO_3 (see the ESI† for details of XPS results of O 1s).[43-45] Therefore, the higher Ce^{3+} ratio of $CeWO_x$ would beneficial for the higher NH_3-SCR activity. In addition, the Ce^{3+} ratio might affect the redox ability and reactants adsorption and activation capacities of the catalysts.

3.5 H_2-TPR

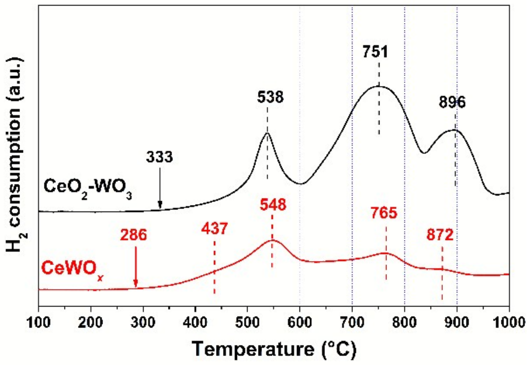

Fig. 5 H_2-TPR profiles of $CeWO_x$ and CeO_2-WO_3 catalysts.

The H_2-TPR profiles of $CeWO_x$ and CeO_2-WO_3 catalysts are shown in Fig. 5. The two peaks at 538/548 and 751/765 °C were associated with the reduction process from WO_3 to WO_2.[46,47] The reduction peak of $CeWO_x$ at 437 °C can be attributed to the reduction of surface Ce^{4+} to Ce^{3+}, while no such a peak was clearly observed for CeO_2-WO_3.[48,49] The peak of the two catalysts at 896/872 °C could be assigned to the reduction of bulk CeO_2. In addition, the onsite H_2 consumption of $CeWO_x$ was observed at 286 °C, which was obviously lower than that of CeO_2-WO_3 at 333 °C. The H_2-TPR profiles strongly suggest a better redox property of $CeWO_x$ than that of CeO_2-WO_3.

A well-known catalytic cycle for the SCR reaction involving both acid-based and redox functions was proposed by Topsøe et al.[50] Previous studies by Lietti et al. have indicated that the redox functions of NH_3-SCR catalyst govern the catalytic reactivity in the low-temperature region.[51,52] Therefore, the superior redox property of $CeWO_x$ due to intense interaction between Ce and W species would beneficial for the low temperature NH_3-SCR activity.

3.6 NO_x/NH_3-TPD

To investigate the NO_x and NH_3 adsorption/desorption capabilities of the catalysts, NO_x-TPD and NH_3-TPD were performed on $CeWO_x$ and CeO_2-WO_3 (Fig. 6).

In the NO_x-TPD profiles in Fig. 6(A), the first NO_x peak at *ca.* 100/125 °C was due to the desorption of physisorbed NO_x, while the second NO_x peak at *ca.* 225/200 °C was mainly associated with the decomposition of chemsorbed NO_x species.[53,54] The additional small peak at *ca.* 400 °C was probably related to the decomposition of bridging nitrate species and bidentate nitrate species with higher thermal stability.[53] The chemsorbed NO_x species on $CeWO_x$ was evidently higher than those on CeO_2-WO_3. In addition, the NO_x adsorption capacity of $CeWO_x$ was 17.9 μmol/g, which was obviously higher than that of CeO_2-WO_3 (9.7 μmol/g). The NO profiles of the two catalysts were similar with those of NO_x. Interestingly, high NO_2 desorption associated with the chemsorbed NO_x species was observed on $CeWO_x$, while almost no NO_2 desorption was observed on CeO_2-WO_3. This result indicates that $CeWO_x$ was more effective for the oxidation of NO to NO_2 and thus enhanced the chemical adsorption of NO_x as nitrate species at low temperature, which is consistent with the separated NO oxidation result. Previous study have shown that NO_x species was mainly adsorbed on Ce sites of Ce-W oxide catalyst during NH_3-SCR reaction.[39] Therefore, more Ce species dispersed on the surface of $CeWO_x$ obtained by homogeneous precipitation method would beneficial for the adsorption and activation of NO_x at low temperature.

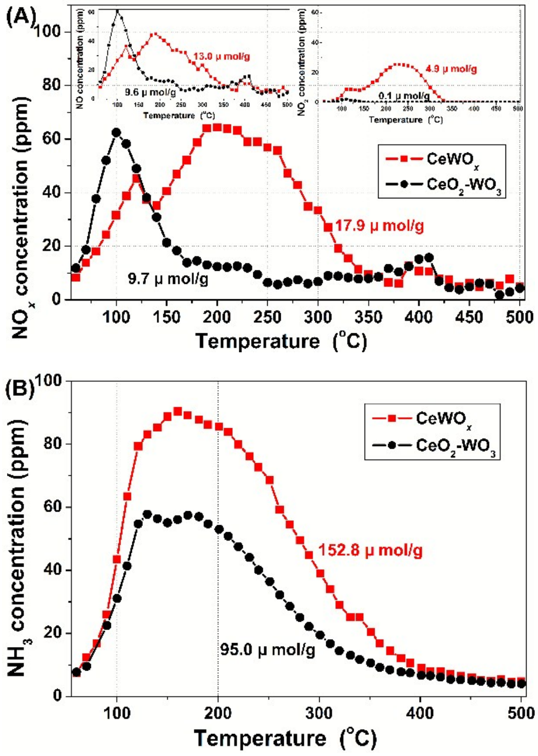

Fig. 6 (A) NO_x-TPD and (B) NH_3-TPD profiles of $CeWO_x$ and CeO_2-WO_3

W has been widely used as an additive for NH_3-SCR catalysts and the effects of W species were attributed to the enhancement of catalyst redox properties and the increase of acid sites.[51,52,55,56] It has been indicated that surface acidity plays an important role in the adsorption and activation of NH_3, and the SCR reaction in the high-temperature region is likely controlled by the surface acid properties.[51,55] In this study, the NH_3 adsorption capacity of $CeWO_x$ (152.8 μmol/g) was clearly higher than that of CeO_2-WO_3 (95.0 μmol/g). When the NH_3 adsorption capacity was normalized by BET surface area, similar results for the two catalysts (2.2 μmol/m² of $CeWO_x$ and 2.4 μmol/m² of CeO_2-WO_3) were obtained, which indicates that the higher NH_3 adsorption capacity of $CeWO_x$ was mainly associated with its higher surface area. The high NH_3 adsorption capacity was probably an important reason for the superior NH_3-SCR activity of $CeWO_x$ at high temperature.

Conclusions

Ce-W oxide catalysts were prepared by homogeneous precipitation method ($CeWO_x$) and solution evaporating method (CeO_2-WO_3). The $CeWO_x$ catalyst was clearly more efficient for NO_x abatement, with higher NO_x conversion (over 80% NO_x conversion from 225 to 450 ^oC under a high GHSV of 300,000 h^{-1}) and lower N_2O production in the whole temperature range.

The BET surface area of $CeWO_x$ was higher than that of CeO_2-WO_3, which is associated with the higher NH_3-SCR activity of $CeWO_x$. The XRD results showed that the coexistence of Ce and W species in $CeWO_x$ could remarkably inhibit the crystallization of CeO_2 and WO_3, which will lead to a high dispersion of active species. The XPS results revealed high Ce^{3+} ratio on $CeWO_x$, which could result in a charge imbalance and thus beneficial for NH_3-SCR reaction. The NO_x-TPD and separate NO oxidation results indicate that $CeWO_x$ is very effective for the oxidation of NO to NO_2 and thus enhance the chemical adsorption of NO_x as nitrate species, which can promote the NH_3-SCR activity at low temperature. The NH_3-TPD results indicate that $CeWO_x$ has outstanding NH_3 adsorption capability, which might be an important reason for the superior NH_3-SCR activity at high temperature.

Based on the above results, we can expect that the $CeWO_x$ catalyst prepared by homogeneous precipitation method can achieve highly dispersed active species and intense interaction between Ce and W species, and thus results in enhanced charge imbalance, superior redox functions, and outstanding adsorption and activation properties of reactants. That is the reason for the excellent NH_3-SCR activity of $CeWO_x$ catalyst.

Acknowledgements

We gratefully acknowledge the financial supports from the National Natural Science Foundation of China (51308296), the Fundamental Research Funds for the Central Universities (30920140111012) and the Qing Lan Project of Jiangsu Province, China.

References

1 Z. Liu and S. Ihl Woo, *Catal. Rev.*, 2006, **48**, 43-89.
2 S. Roy, M. S. Hegde and G. Madras, *Appl. Energ.*, 2009, **86**, 2283-2297.
3 G. Busca, L. Lietti, G. Ramis and F. Berti, *Appl. Catal., B*, 1998, **18**, 1-36.
4 P. Granger and V. I. Parvulescu, *Chem. Rev.*, 2011, 111, 3155-3207.
5 F. Liu, Y. Yu and H. He, *Chem. Commun.*, 2014, **50**, 8445-8463.
6 M. Koebel, M. Elsener and M. Kleemann, *Catal. Today*, 2000, 59, 335-345.
7 B. Guan, R. Zhan, H. Lin and Z. Huang, *Appl. Therm. Eng.*, 2014, **66**, 395-414.
8 F. Liu, W. Shan, D. Pan, T. Li and H. He, *Chin. J. Catal.*, 2014, **35**, 1438-1445.
9 S. Brandenberger, O. Kröcher, A. Tissler and R. Althoff, *Catal. Rev.*, 2008, **50**, 492-531.
10 R. Q. Long and R. T. Yang, *J. Am. Chem. Soc.*, 1999, **121**, 5595-5596.
11 A. Z. Ma and W. Grunert, *Chem. Commun.*, 1999, 71-72.
12 J. H. Kwak, R. G. Tonkyn, D. H. Kim, J. Szanyi and C. H. F. Peden, *J. Catal.*, 2010, **275**, 187-190.
13 L. Ren, L. Zhu, C. Yang, Y. Chen, Q. Sun, H. Zhang, C. Li, F. Nawaz, X. Meng and F.-S. Xiao, *Chem. Commun.*, 2011, **47**, 9789-9791.
14 D. W. Fickel, E. D'Addio, J. A. Lauterbach and R. F. Lobo, *Appl. Catal., B*, 2011, **102**, 441-448.
15 R. Martínez-Franco, M. Moliner, C. Franch, A. Kustov and A. Corma, *Appl. Catal., B*, 2012, **127**, 273-280.
16 M. Moliner, C. Franch, E. Palomares, M. Grill and A. Corma, *Chem. Commun.*, 2012, **48**, 8264-8266.
17 R. Martínez-Franco, M. Moliner and A. Corma, *J. Catal.*, 2014, **319**, 36-43.
18 W. Shan and H. Song, *Catal. Sci. Technol.*, 2015, **5**, 4280-4288.
19 U. Deka, I. Lezcano-Gonzalez, B. M. Weckhuysen and A. M. Beale, *ACS Catal.*, 2013, 413-427.
20 F. Gao, J. Kwak, J. Szanyi and C. F. Peden, *Top. Catal.*, 2013, **56**, 1441-1459.
21 F. Liu, H. He and C. Zhang, *Chem. Commun.*, 2008, 2043-2045.
22 Z. Si, D. Weng, X. Wu, J. Li and G. Li, *J. Catal.*, 2010, **271**, 43-51.
23 M. Casapu, O. Kröcher and M. Elsener, *Appl. Catal., B*, 2009, **88**, 413-419.
24 Y. J. Kim, H. J. Kwon, I.-S. Nam, J. W. Choung, J. K. Kil, H.-J. Kim, M.-S. Cha and G. K. Yeo, *Catal. Today*, 2010, **151**, 244-250.
25 W. Shan, F. Liu, Y. Yu and H. He, *Chin. J. Catal.*, 2014, **35**, 1251-1259.
26 W. Shan, F. Liu, H. He, X. Shi and C. Zhang, *Chem. Commun.*, 2011, **47**, 8046-8048.
27 W. Shan, F. Liu, H. He, X. Shi and C. Zhang, *ChemCatChem*, 2011, **3**, 1286-1289.
28 H. Huang, W. Shan, S. Yang and J. Zhang, *Catal. Sci. Technol.*, 2014, **4**, 3611-3614.
29 W. Shan, F. Liu, H. He, X. Shi and C. Zhang, *Catal. Today*, 2012, **184**, 160-165.
30 W. Shan, F. Liu, Y. Yu, H. He, C. Deng and X. Zi, *Catal. Commun.*, 2015, **59**, 226-228.
31 C. H. Kim, G. Qi, K. Dahlberg and W. Li, *Science*, **327**, 1624-1627.
32 W. Yang, Q. Liu, W. Qiu, S. Lu and L. Yang, *Solid State Ionics*, 1999, **121**, 79-84.
33 G. Qi and R. T. Yang, *Chem. Commun.*, 2003, 848-849.
34 P. Hu, Z. Huang, W. Hua, X. Gu and X. Tang, *Appl. Catal., A*, 2012, **437-438**, 139-148.
35 Z. Huang, Z. Zhu and Z. Liu, *Appl. Catal., B*, 2002, **39**, 361-368.
36 J. Li, H. Chang, L. Ma, J. Hao and R. T. Yang, *Catal. Today*, 2011, **175**, 147-156.
37 F. Liu, W. Shan, Z. Lian, L. Xie, W. Yang and H. He, *Catal. Sci. Technol.*, 2013, **3**, 2699-2707.
38 G. Qi and R. T. Yang, *Appl. Catal., B*, 2003, **44**, 217-225.
39 Y. Peng, K. Li and J. Li, *Appl. Catal., B*, 2013, **140–141**, 483-492.
40 C. Liu, L. Chen, H. Chang, L. Ma, Y. Peng, H. Arandiyan and J. Li, *Catal. Commun.*, 2013, **40**, 145-148.
41 Z. Liu, Y. Yi, J. Li, S. I. Woo, B. Wang, X. Cao and Z. Li, *Chem. Commun.*, 2013, **49**, 7726-7728.
42 T. Gu, Y. Liu, X. Weng, H. Wang and Z. Wu, *Catal. Commun.*, 2010, **12**, 310-313.
43 J.-C. Dupin, D. Gonbeau, P. Vinatier and A. Levasseur, *Phys. Chem. Chem. Phys.*, 2000, **2**, 1319-1324.
44 D. Y. Yoon, E. Lim, Y. J. Kim, J. H. Kim, T. Ryu, S. Lee, B. K. Cho, I.-S. Nam, J. W. Choung and S. Yoo, *J. Catal.*, 2014, **319**, 182-193.

45 C. Zhang, C. Wang, W. Zhan, Y. Guo, Y. Guo, G. Lu, A. Baylet and A. Giroir-Fendler, *Appl. Catal., B*, 2013, **129**, 509-516.
46 Z. Ma, D. Weng, X. Wu, Z. Si and B. Wang, *Catal. Commun.*, 2012, **27**, 97-100.
47 D. G. Barton, S. L. Soled, G. D. Meitzner, G. A. Fuentes and E. Iglesia, *J. Catal.*, 1999, **181**, 57-72.
48 L. Chen, J. Li and M. Ge, *J. Phys. Chem. C*, 2009, **113**, 21177-21184.
49 Z. Liu, S. Zhang, J. Li and L. Ma, *Appl. Catal., B*, 2014, **144**, 90-95.
50 N.-Y. Topsøe, *Science*, 1994, **265**, 1217-1219.
51 L. Lietti, I. Nova and P. Forzatti, *Top. Catal.*, 2000, **11-12**, 111-122.
52 L. Lietti, P. Forzatti and F. Berti, *Catal. Lett.*, 1996, **41**, 35-39.
53 F. Liu and H. He, *J. Phys. Chem. C*, 2010, **114**, 16929-16936.
54 F. Liu, H. He, Y. Ding and C. Zhang, *Appl. Catal., B*, 2009, **93**, 194-204.
55 L. Lietti, P. Forzatti and F. Bregani, *Ind. Eng. Chem. Res.*, 1996, **35**, 3884-3892.
56 J. P. Chen and R. T. Yang, *Appl. Catal., A*, 1992, **80**, 135-148.

Graphical Abstract

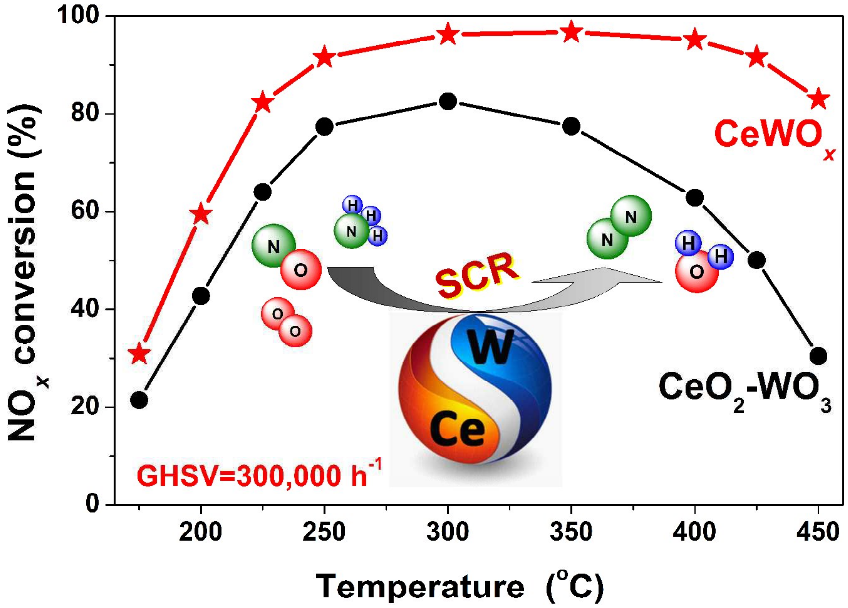

Characterizations were used to investigate the main reason for the high efficient NO_x abatement by $CeWO_x$ catalyst.